FEBS Letters 582 (2008) 1459–1464

Small mitochondrial ARF (smARF) is located in both the nucleus and cytoplasm, induces cell death, and activates p53 in mouse fibroblasts

Yuko Ueda[1], Terutsugu Koya[1], Noriko Yoneda-Kato, Jun-ya Kato*

Graduate School of Biological Sciences, Nara Institute of Science and Technology, 8916-5 Takayama, Ikoma, Nara 630-0101, Japan

Received 20 January 2008; revised 10 March 2008; accepted 19 March 2008

Available online 31 March 2008

Edited by Varda Rotter

Abstract **The ARF transcript produces two proteins, the full-length ARF, $p19^{ARF}$, and a short mitochondrial version, smARF. To explore the functional difference between the two, we generated GFP-fused expression vectors for each protein and introduced them into NIH3T3 murine fibroblasts, which sustains a global deletion in the INK4a locus but contains a functional p53 gene. GFP-$p19^{ARF}$ was located within the nucleolus as previously reported, whereas GFP-smARF was detected mainly in the nucleoplasm. GFP-smARF induced cell death although to a slightly lesser extent than $p19^{ARF}$. GFP-smARF stabilized p53 thereby inducing expression of the target genes, MDM2 and p21. We suggest that smARF has functions other than mitochondria-mediated autophagy, and induces p53 expression and cell death via a novel mechanism.**

Keywords: smARF; p53; Nuclear localization; MDM2

1. Introduction

The tumor suppressor gene locus INK4a encodes two different proteins, $p16^{INK4a}$ and ARF [1]. $p16^{INK4a}$ functions as a Cdk inhibitor, binding to and inhibiting the activity of cyclin D-dependent kinases, Cdk4 and Cdk6, thereby regulating the action of the tumor suppressor, a retinoblastoma (pRb) protein [2]. ARF ($p19^{ARF}$ and $p14^{ARF}$ for the mouse and human proteins, respectively), on the other hand, negatively regulates the activity of the ubiquitin ligase MDM2 and inhibits the degradation of another tumor suppressor, p53 [3]. Therefore, the INK4a locus plays a critical role in tumor suppression by regulating the two major tumor suppressor proteins, pRb and p53. Consistent with this idea, the INK4a locus is, in fact, frequently deleted or epigenetically suppressed in a variety of human cancers [4,5].

In addition to the regulation of the MDM2-p53 pathway, ARF is suggested to play a role in cell proliferation control in a p53-independent manner [6]. For example, ARF is still capable of inhibiting the proliferation of $p53^{-/-}MDM2^{-/-}$ cells although somewhat less effectively than in wild-type control cells. $ARF^{-/-}p53^{-/-}MDM2^{-/-}$ mice develop tumors at a frequency slightly but definitely higher than that of $p53^{-/-}MDM2^{-/-}$ animals [7]. Therefore, it is evident that ARF can control cell proliferation in a p53-independent manner as well. Although the precise pathway has yet to be clarified, several possible mechanisms have been suggested. ARF regulates ribosome biosynthesis [8] partially by binding to and regulating nucleophosmin (NPM) [9–11]. ARF regulates the activity of several transcription factors including myc by direct binding [12]. Besides MDM2, ARF binds to and regulates the activity of another ubiquitin ligase, ARF-BP1 or Mule [13], which triggers degradation of several target proteins including myc besides p53, some of which may be responsible for p53-independent cell proliferation. Furthermore, it is reported that the ARF transcript produces a shorter version of the protein in addition to the full-length $p19^{ARF}$ polypeptide, which starts from the internal methionine Met at position 45 and predominantly distributes in the mitochondria: this truncated form has been designated short mitochondrial ARF (smARF) [14]. smARF lacks the MDM2-binding domain located in the N-terminus, and is suggested to play a role in autophagy in a p53-independent manner. In this study, we explored the intracellular function of smARF to control cell proliferation. We fused smARF with GFP, introduced it into NIH3T3 cells, which sustain a wide range of deletions at the INK4a gene locus, but contain a wild-type allele of p53 gene, and examined its intracellular sublocalization and the effect on cell proliferation and survival.

2. Materials and methods

2.1. Cell culture and transfection

NIH3T3 (Arf-null, p53-wild-type) mouse fibroblasts, 293T human embryonic kidney cells, and HeLa human cervical carcinoma cells were cultured in Dulbecco's modified Eagle's medium (DMEM) supplemented with 10% fetal bovine serum (FBS), 2 mM glutamine, 100 U/ml of penicillin, and 100 μg/ml of streptomycin (GIBCO/BRL), and transfected with expression vectors via the calcium phosphate-DNA precipitation method [15].

2.2. Plasmid construction

We constructed a GFP-fusion protein expression vector (pMSCV-puro-GFP) [16] by modifying the retroviral vector pMSCV-IRES-puro (Clontech). cDNA fragments containing the coding sequence of smARF (Cdkn2a, smARF variant, GenBank accession number EU071702) and the full-length p19ARF (Cdkn2a, variant 1, p19ARF, GenBank accession number NM009877) were subcloned into the pMSCV-puro-GFP vector in-frame with GFP.

2.3. Protein analyses

Cell lysis, immunoprecipitation, sodium dodecyl sulfate–polyacrylamide gel electrophoresis (SDS–PAGE), and immunoblotting were performed as described [16,17]. In short, cells were washed with PBS and lysed for 30 min on ice in modified EBC buffer (50 mM Tris–HCl, pH

*Corresponding author. Fax: +81 743 72 5519.
E-mail address: jkata@bs.naist.jp (J. Kato).

[1]These authors contributed equally to this work.

0014-5793/$34.00
doi:10.1016/j.febslet.2008.03.032

8.0, 120 mM NaCl, 1 mM EDTA, and 0.5% NP40) containing 2000 KIU/ml of aprotinin, 1 mM PMSF, 0.1 mM NaF, 0.1 mM Na_3VO_4, and 10 mM β-glycerophosphate. The cell debris was removed by micro centrifugation at full speed. The antibodies were reacted with cell lysates for 2 h to overnight at 4 °C. Immune complexes were collected by incubation with protein A or protein G Sepharose beads for 2 h at 4 °C, and boiled in SDS-sample buffer (40 mM Tris–HCl, pH 6.8, 0.1 M DTT, 1% SDS, 10% glycerol, and 0.05% bromophenol blue) for 4 min. To prepare direct lysates for immunoblotting, cell lysates in a EBC buffer were mixed with the same amount of 2× SDS-sample buffer (80 mM Tris–HCl, pH 6.8, 0.2 M DTT, 2% SDS, 20% glycerol, and 0.1% bromophenol blue) and boiled for 4 min. Protein samples were separated on SDS–polyacrylamide gels under reducing conditions (SDS–PAGE), transferred to a nitrocellulose membrane or a PVDF membrane (Millipore), and immunoblotted with the antibodies indicated. Proteins were detected with the ECL blotting system (Amersham) according to the manufacturer's instructions. Developed films were quantitatively analyzed with a densitograph (ATTO, Japan).

Rabbit polyclonal antibodies to p53 (FL-393) and Grb2 (C-23) and a goat polyclonal antibody to p21 (C-19) were purchased from Santa Cruz Biotechnology. A mouse monoclonal antibody to γ-tubulin (GTU-88) and a rabbit polyclonal antibody to $p19^{ARF}$(Ab80) were obtained from Sigma and Abcam, respectively. Rabbit polyclonal antibodies to p53 and p21 were generated using bacterially produced polypeptides in our laboratory. A mouse monoclonal antibody to MDM2 was provided by Dr. Arnold J. Levine. Rabbit polyclonal antibody to GFP (BD Living Colors) was from BD Biosciences. Mouse monoclonal antibody to an HA epitope (clone 12CA5) was purchased from Boehringer Mannheim.

2.4. Immunofluorescence staining

For the analysis of the subcellular localization of GFP-fused proteins, NIH3T3, 293T, and HeLa cells were photographed by fluorescence (GFP) microscopy (Olympus, Japan) at 48–72 h after transfection. For the immunofluorescence staining, cells were grown on glass slides, fixed in 4% paraformaldehyde, permeabilized in 0.5% Triton X-100, stained with cell culture supernatant containing the mouse monoclonal antibody indicated and incubated with fluorescein-linked anti-mouse IgG (Amersham). Chromosomal DNA was stained by incubation in 1 μg/ml of Hoechst 33342 for 2 min. The samples were viewed by phase-contrast or fluorescence microscopy.

2.5. Flow cytometric analysis

For the cell cycle analysis, cells were stained with a 1 ml solution of 0.1% sodium citrate and 0.1% Triton X-100 containing 50 μg/ml of propidium iodide and treated with 1 μg/ml of RNase for 30 min at room temperature. Fluorescence from the propidium iodide–DNA complex was measured with a FACScan flow cytometer (Becton Dickinson), and the percentage of cells in the sub-G1 population was determined with Modifit cell cycle software. The populations of dead cells were confirmed by the dye exclusion assay.

2.6. Cell fractionation

To perform the nuclear-enriched fractionation, cells were suspended on ice in 0.1% NP40 buffer (10 mM HEPES–KOH, pH 7.8, 10 mM KCl, 0.1 mM EDTA, and 0.1% NP40) supplemented with 0.1 mM Na_3VO_4, 0.1 mM NaF, 10 mM β-glycerophosphate, 2% aprotinin, and 0.5% PMSF, homogenized by multiple passages through a 27 G needle, incubated for 5 min on ice, and centrifuged at $2000 \times g$ for 2 min at 4 °C to pellet the nuclear fraction. The supernatant was recovered as a cytoplasmic fraction (designated as N/C because this fraction contained some nuclear fraction). The pelleted nuclear fraction was extracted by homogenizing 10 passages through a 27 G needle in modified EBC buffer supplemented with inhibitors, incubated for 1 h on ice, and centrifuged at $18\,000 \times g$ for 10 min at 4 °C. The resulting supernatant was collected as a final nuclear fraction (designated as N). Direct lysate as described above was used as the whole cell fraction (W).

3. Results

To visualize the intracellular behavior of the smARF protein, we constructed a vector that expresses the GFP-fused smARF protein. We subcloned smARF cDNA in-frame with green fluorescent protein (GFP) into the mammalian expression vector, pMSCV-puro-GFP [16], which expresses inserted cDNA as the GFP-fusion protein under the control of the MSCV promoter and contains the puromycin resistance gene as a selection marker. As a control, we introduced full-length $p19^{ARF}$ cDNA into the same vector in place of smARF cDNA.

The mouse fibroblast cell line, NIH3T3, was used for the following analysis because this cell line contains a global deletion in the INK4a locus and expresses neither $p16^{INK4a}$ nor $p19^{ARF}$ (not smARF neither). But these cells retain the normal allele of the p53 gene and in response to UV, γ-ray, and DNA-damaging reagents (alkylating chemicals), activation of p53 swiftly occurs resulting in the induction of downstream target genes such as p21 and MDM2 (data not shown but see [16]).

NIH3T3 cells were transfected with the expression vectors (pMSCV-puro-GFP-smARF, pMSCV-puro-GFP-$p19^{ARF}$, and an empty vector, pMSCV-puro-GFP) by the calcium phosphate precipitation technique [15]. The cells were harvested at 48 h post transfection, and the cell lysates were analyzed by Western blotting with the specific antibodies indicated (Fig. 1A). An antibody to GFP readily recognized GFP and GFP-fused proteins (GFP-$p19^{ARF}$ and GFP-smARF). The antibody specific to the C-terminus of mouse ARF detected GFP-fusion proteins of the same molecular weight. Importantly, neither antibody detected any species with a smaller molecular weight, indicating that degradation of the ectopically expressed protein was under the detectable level, and the GFP-signal is from the full-length fusion protein and not from the truncated protein. In the lysate from the GFP-$p19^{ARF}$-transfected cells, we did not detect the polypeptide with the lower molecular weight (ca 14 kDa, corresponding to smARF) using the antibody recognizing both $p19^{ARF}$ and smARF. It is likely that smARF protein is not produced from the GFP-$p19^{ARF}$ transcript.

To explore the intracellular behavior of the smARF protein, we examined NIH3T3 cells transfected with the GFP vectors (pMSCV-puro-GFP-smARF, pMSCV-puro-GFP-$p19^{ARF}$, and an empty vector, pMSCV-puro-GFP) under the fluorescent microscope (Fig. 2A). The GFP signal in pMSCV-puro-GFP-transfected cells was observed throughout cell but was slightly stronger in the nucleus, showing no sign of specific intracellular localization, while the GFP signal in pMSCV-puro-GFP-$p19^{ARF}$-transfected cells was compartmentalized within the nucleolus, consistent with the report that $p19^{ARF}$ is located in the nucleolus. The GFP signal in pMSCV-puro-GFP-smARF-transfected cells was, however, unexpectedly detected mostly in the nucleus, some being in the cytoplasm, but did not specifically localize within the mitochondria. Because Western blotting data confirmed that there is little degradation product (Fig. 1A), the GFP signal we observed most probably reflects that of GFP-smARF. After counting the cells with different intracellular localization of the GFP signal, the results clearly showed that GFP-smARF mostly resided in the nucleoplasm but was occasionally found in the nucleolus as well (Fig. 2B), a clear distinction from the distribution of the full-length $p19^{ARF}$.

Because the nuclear localization of the GFP-smARF protein was unexpected, we investigated whether this is specific to mouse fibroblasts. We transfected the cell lines, human embryonic kidney-derived HEK293T cells and human cervical carcinoma-derived HeLa cells with the same set of vectors

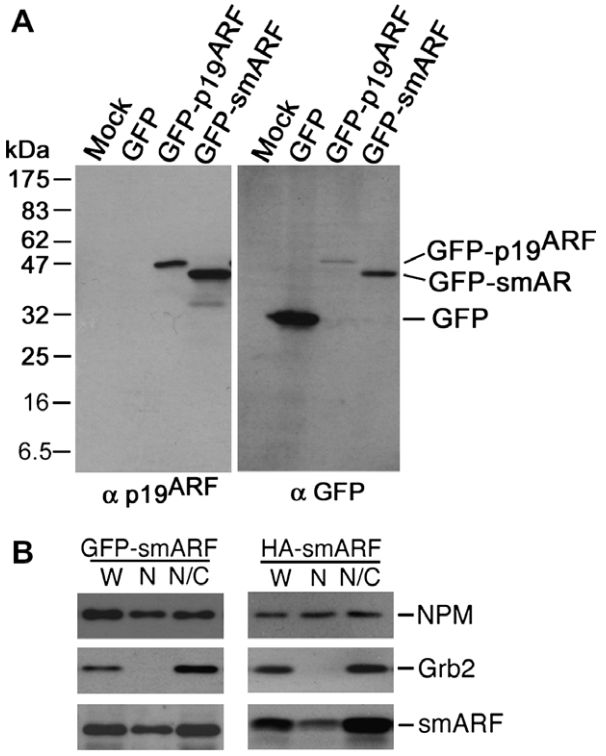

Fig. 1. Expression of GFP-tagged p19^{ARF} and smARF and subcellular localization of smARF. (A) NIH3T3 cells were mock-transfected (Mock) or transfected with vectors encoding GFP, GFP-tagged p19^{ARF} (GFP-p19^{ARF}), and GFP-tagged smARF (GFP-smARF). Cells were harvested at 48 h post-transfection and the lysates were subjected to immunoblotting with antibodies specifically recognizing C-terminus ARF (Left panel, αp19ARF) and GFP (αGFP). The positions of GFP-p19^{ARF}, GFP-smARF, and GFP are shown at the right of the panels. The positions of the molecular weight markers are indicated at the left of the panels. (B) NIH3T3 cells were transfected with vectors encoding GFP-smARF and HA-smARF. Cells were harvested at 48 h post-transfection and extracted to yield the nuclear fraction (N) and the fraction containing both nuclei and cytoplasm (N/C). The lysates (20 μg) were subjected to immunoblotting with antibodies specifically recognizing nucleophosmin (NPM, marker for nuclear protein), Grb2 (marker for cytoplasmic protein), and C-terminus ARF. The position of each protein is shown at the right of the panel. W: whole cell lysate (ca 60% of N and N/C fractions were loaded in the lane).

(pMSCV-puro-GFP-smARF, pMSCV-puro-GFP-p19^{ARF}, and an empty vector, pMSCV-puro-GFP) and examined the subcellular localization of the GFP signal (Fig. 2C, and data not shown). Again we found GFP-smARF largely in the nucleus. Thus, we conclude that smARF harbors nuclear transport potential.

smARF was reported to be transported into the mitochondria and induce cell death by autophagy [14]. Since we found GFP-smARF mainly in the nucleus, we investigated the effect of exogenously expressed GFP-smARF on the survival of ARF-null NIH3T3 mouse fibroblasts. NIH3T3 cells were transfected with the expression vectors (pMSCV-puro-GFP-smARF, pMSCV-puro-GFP-p19^{ARF}, and an empty vector, pMSCV-puro-GFP) and selected in medium containing puromycin. Under these conditions, numerous colonies appeared in the GFP vector-transfected culture, but few colonies grew in the cultures transfected with GFP-smARF and GFP-p19^{ARF}. To determine whether this is due to loss of cell viability, we analyzed cell viability by FACS at 48 h post-transfection without selection in puromycin. To attempt to analyze the possibly early event after expression of the transduced gene rather than the late event, we harvested cells as early as 48 h post-transfection. Fig. 3 shows that transfection of GFP-p19^{ARF} vector resulted in cell death after 48 h. The frequency of cell death was even higher later during the culture. The introduction of GFP-smARF also induced cell death at this time point although slightly less efficiently than that of GFP-p19^{ARF}. Similar results were obtained in the trypan blue dye exclusion assay and when we used HA-tagged constructs. Given that the protein expression was stronger for GFP-smARF than GFP-p19^{ARF}, full-length p19^{ARF} induces cell death more efficiently. However, the results clearly show that nuclear smARF is capable of inducing cell death.

p19^{ARF} is known to activate p53 by directly binding to and inhibiting the ubiquitin ligase MDM2 [18,19], whereas smARF is reported not to do so [14]. Because we found GFP-smARF in the nucleus, we examined whether the expression of GFP-smARF has any impact on the MDM2-p53 pathway. NIH3T3 cells were transfected with the expression vectors (pMSCV-puro-GFP-smARF, pMSCV-puro-GFP-p19^{ARF}, and an empty vector, pMSCV-puro-GFP) and harvested after 48 h. Cell lysates were analyzed by Western blotting with antibodies specific to p53, p21, and MDM2 (Fig. 4A). Transfection of GFP-p19^{ARF} activated p53 by increasing the level of p53, thereby inducing the expression of downstream target genes such as p21 and MDM2. Surprisingly, we observed an increase of p53 expression in cells transfected with GFP-smARF. The p53 appeared to be active because the downstream targets p21 and MDM2 were also activated.

In order to examine the nuclear localization of GFP-smARF by a different approach, we performed cell fractionation experiments. In a previously reported experiment, the nuclear fraction was contaminated by a certain amount of the cytoplasmic fraction [14], which prevented the obtaining of a clear conclusion. We obtained two fractions: (1) a nuclear fraction (designated as N) that exclusively contained extracts from nuclei and (2) the nuclear/cytoplasmic fraction (designated as N/C) that contained both nuclear and cytoplasmic fractions. Each fraction was analyzed by Western blotting with antibodies specifically recognizing nuclear protein (nucleophosmin, NPM), cytoplasmic protein (Grb2), and the C-terminal portion of ARF protein (therefore, recognizing both full-length p19^{ARF} and smARF). We also used the expression vector for HA-tagged smARF to reduce the size-effect of tagging. Fig. 1B shows that the nuclear fraction (N) was pure enough to be free from the cytoplasm because we did not detect any Grb2 protein. GFP-smARF was detected in both the N and N/C fractions, consistent with the results obtained by fluorescent microscopy. As expected, we detected HA-tagged smARF protein in both the N and N/C fractions, indicating that regardless of the different tags, smARF is capable of locating in the nucleus as well as in the cytoplasm.

Because we found a fraction of smARF in the nucleus, we decided to examine whether smARF and MDM2 may form a stable complex in the cell by performing immunoprecipitation followed by Western blotting. Because our antibody to GFP is not well suited for immunoprecipitation, we decided to use an antibody to the HA tag. NIH3T3 cells were transfected with expression vectors for HA-p19^{ARF} and HA-smARF, harvested after 48 h, and immunoprecipitated with a mouse monoclonal

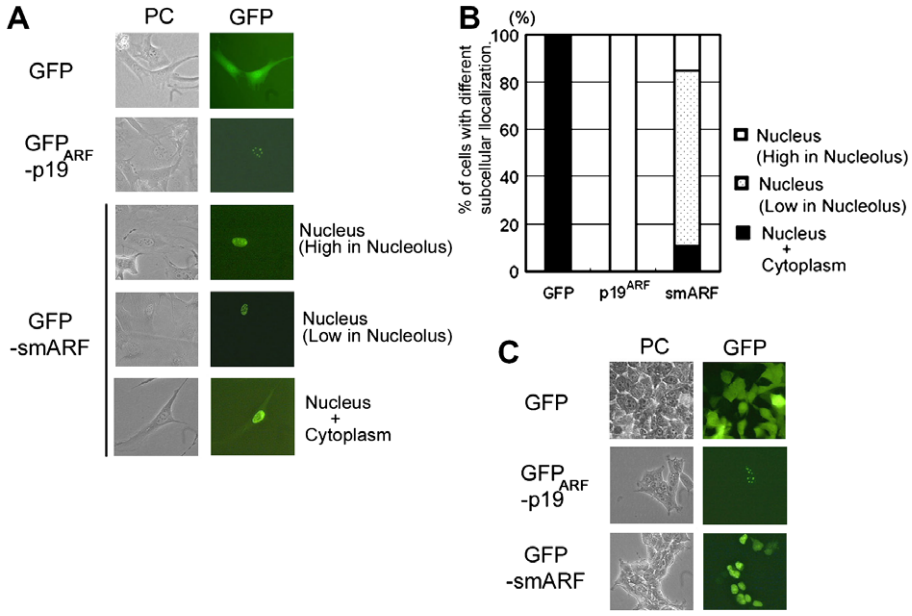

Fig. 2. Subcellular localization of the GFP-tagged proteins in mouse fibroblasts and human cells. (A) NIH3T3 cells were transfected with vectors encoding GFP, GFP-p19^{ARF}, and GFP-smARF, and were examined under the fluorescence microscope at 48 h post-transfection. PC: phase contrast. (B) More than 500 cells transfected with vectors encoding GFP, GFP-p19^{ARF}, and GFP-smARF were examined and enumerated under the fluorescence microscope at 48 h post-transfection. Data are shown as the percentage of the number of cells exhibiting different localization of the GFP signal. (C) HEK293T cells were transfected with vectors encoding GFP, GFP-p19^{ARF}, and GFP-smARF, and were examined under the fluorescence microscope at 48 h post-transfection. PC: phase contrast.

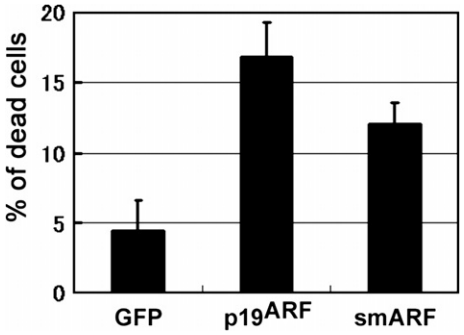

Fig. 3. Induction of cell death by GFP-tagged p19^{ARF} and smARF. NIH3T3 cells were transfected with vectors encoding GFP, GFP-p19^{ARF}, and GFP-smARF. Cells were harvested at 48 h post-transfection and analyzed for cell death by FACS. Similar results were obtained by the dye exclusion assay and when we used HA-tagged constructs. In all cases, the difference is significant ($P < 0.005$).

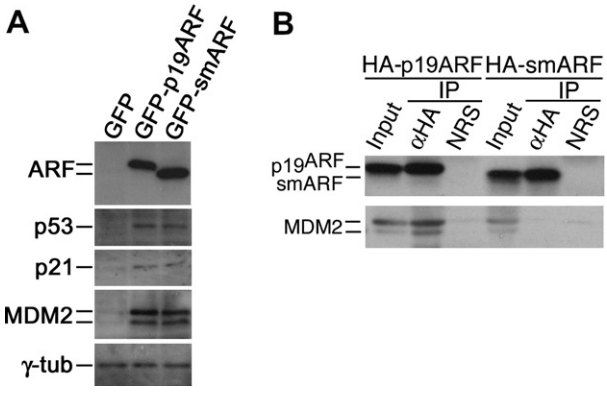

Fig. 4. Activation of p53 and interaction with MDM2 by p19^{ARF} and smARF. (A) NIH3T3 cells were transfected with vectors encoding GFP, GFP-p19^{ARF}, and GFP-smARF. Cells were harvested at 48 h post-transfection and the lysates were subjected to immunoblotting with antibodies specifically recognizing ARF, p53, p21, MDM2, and γ-tubulin. The position of each protein is shown at the left of each panel. (B) NIH3T3 cells were transfected with vectors encoding HA-p19^{ARF} and HA-smARF, and harvested at 48 h post-transfection. p19^{ARF} and smARF proteins were immunoprecipitated from the cell lysates 100 μg) with antibody (2 μg) specifically recognizing HA-tag. The immunoprecipitates were subjected to immunoblotting with antibodies to C-terminus ARF and MDM2. The positions of HA-p19^{ARF}, HA-smARF, and MDM2 are shown at the left of the panels. Input: ca 30% of cell lysate used for immunoprecipitation was loaded in the lane.

antibody specifically recognizing the HA tag and a control antibody (NRS). The precipitates were separated on SDS–PAGE gels and analyzed by Western blotting using antibodies to the C-terminus of ARF and MDM2. As expected, MDM2 was found in an anti-HA immunoprecipitate of the lysate from cells transfected with HA-tagged full-length ARF (HA-p19^{ARF}), while little MDM2 was detected in an anti-HA immunoprecipitate from the HA-smARF-transfected cells (Fig. 4B). The level of MDM2 was slightly lower in smARF transfectants but the quantitative analysis showed that more than 50% of the MDM2 protein bound to p19^{ARF}, whereas less than 5% of MDM2 was found to be in a complex with smARF. Thus, as previously reported [14], smARF showed a much lower affinity for interaction with MDM2 in vivo.

4. Discussion

In the present study, we investigated the intracellular actions of smARF, which was previously reported to be located in the mitochondria and induce cell death by autophagy [14]. To our

surprise, we detected the GFP-signal in the nucleus (largely in the nucleoplasm) of the mouse fibroblasts transfected with the vector that allows expression of the GFP-tagged smARF protein. The signal seems to reflect that of the GFP-smARF fusion protein because we did not detect any degradation intermediates in the Western blot analysis using two different antibodies. This does not seem to be a cell type- or species-specific phenomenon because we found the nuclear GFP-smARF in human HEK293T and HeLa cells as well.

It is possible that the GFP-tagging affects the subcellular localization of smARF because the GFP (ca 27 kDa) is significantly larger than smARF itself (ca 14 kDa), but cell fractionation experiments revealed that smARF with a much smaller tag such as an HA-tag was also present in the nucleus. smARF was found in the mitochondria by immunofluorescent staining [14]. However, it is highly probable that smARF forms a complex with other molecules in the nucleus and considering the small size of the smARF protein, the possibility cannot be excluded that the epitope in smARF is masked by interaction with other molecules. In the cell fractionation experiment, the nuclear fraction was highly contaminated with unlysed cells and it was almost impossible to tell whether smARF is in the nucleus or not. To clarify this point, we modified the fractionation protocol to eliminate the unlysed cells and found smARF (both GFP-smARF and HA-smARF) in the nucleus. Thus, we conclude that smARF can be transported into the nucleus. Consistent with our results, previous reports analyzing ARF function with deletion mutants showed that the N-terminus ARF mutants, especially the one lacking the first 62 amino acids, were excluded from the nucleolus, but still in the nucleoplasm and cytoplasm [20–22].

If smARF is located in the nucleus, what is its physiological function? Because smARF lacks the domain mainly required for interaction with MDM2, it is unlikely that smARF regulates the activity of this ubiquitin ligase. However, given that smARF is still capable of inducing the expression of p53, although much less so than full-length $p19^{ARF}$, smARF may still be able to bind to MDM2 with a lower affinity using an additional MDM2 binding motif, which was originally found in human $p14^{ARF}$[23], or, alternatively, may interact with and regulate other ubiquitin ligases for p53 such as ARF-BP1 [13], Pirh2 [24], and COP1 [25]. Other possibility is that smARF may functionally interact with nucleophosmin (NPM) [9–11] and modulate its associated functions to control cell proliferation and survival. Further studies will be required to clarify these possibilities. Another issue is that if smARF functions both in the mitochondria and in the nucleus, it is feasible that smARF shuttles between the nucleus and the cytoplasm (mitochondria) and GFP-tagging interferes with the nuclear export of smARF. Because p53 is reported to be exported from the nucleus before degradation [26] or even transported into the mitochondria [27] to induce apoptosis or autophagy, this possibility should also be tested in the future.

Acknowledgements: We thank Dr. J. Fujisawa for the plasmid, Drs. C.J. Sherr and M.F. Roussel for the NIH3T3 cell line, Drs. K. Tago and H. Itoh for advice on cell fractionation, and Ms. I. Nakamae for excellent technical assistance. This work was partly supported by Grants-in-Aid for Scientific Research and for Cancer Research from the Ministry of Education, Science, and Culture of Japan.

References

[1] Quelle, D.E., Zindy, F., Ashmun, R.A. and Sherr, C.J. (1995) Alternative reading frames of the INK4a tumor suppressor gene encode two unrelated proteins capable of inducing cell cycle arrest. Cell 83, 993–1000.
[2] Sherr, C.J. (2004) Principles of tumor suppression. Cell 116, 235–246.
[3] Sherr, C.J. and Weber, J.D. (2000) The ARF/p53 pathway. Curr. Opin. Genet Dev. 10, 94–99.
[4] Ruas, M. and Peters, G. (1998) The p16INK4a/CDKN2A tumor suppressor and its relatives. Biochim. Biophys. Acta 1378, F115–F177.
[5] Sharpless, N.E. (2005) INK4a/ARF: a multifunctional tumor suppressor locus. Mutat. Res. 576, 22–38.
[6] Sherr, C.J. et al. (2005) p53-Dependent and -independent functions of the Arf tumor suppressor. Cold Spring Harb. Symp. Quant. Biol. 70, 129–137.
[7] Weber, J.D., Jeffers, J.R., Rehg, J.E., Randle, D.H., Lozano, G., Roussel, M.F., Sherr, C.J. and Zambetti, G.P. (2000) p53-independent functions of the p19(ARF) tumor suppressor. Genes Dev. 14, 2358–2365.
[8] Sugimoto, M., Kuo, M.L., Roussel, M.F. and Sherr, C.J. (2003) Nucleolar Arf tumor suppressor inhibits ribosomal RNA processing. Mol. Cell 11, 415–424.
[9] Bertwistle, D., Sugimoto, M. and Sherr, C.J. (2004) Physical and functional interactions of the Arf tumor suppressor protein with nucleophosmin/B23. Mol. Cell Biol. 24, 985–996.
[10] Korgaonkar, C., Hagen, J., Tompkins, V., Frazier, A.A., Allamargot, C., Quelle, F.W. and Quelle, D.E. (2005) Nucleophosmin (B23) targets ARF to nucleoli and inhibits its function. Mol. Cell Biol. 25, 1258–1271.
[11] Itahana, K., Bhat, K.P., Jin, A., Itahana, Y., Hawke, D., Kobayashi, R. and Zhang, Y. (2003) Tumor suppressor ARF degrades B23, a nucleolar protein involved in ribosome biogenesis and cell proliferation. Mol. Cell 12, 1151–1164.
[12] Qi, Y., Gregory, M.A., Li, Z., Brousal, J.P., West, K. and Hann, S.R. (2004) p19ARF directly and differentially controls the functions of c-Myc independently of p53. Nature 431, 712–717.
[13] Chen, D., Kon, N., Li, M., Zhang, W., Qin, J. and Gu, W. (2005) ARF-BP1/Mule is a critical mediator of the ARF tumor suppressor. Cell 121, 1071–1083.
[14] Reef, S., Zalckvar, E., Shifman, O., Bialik, S., Sabanay, H., Oren, M. and Kimchi, A. (2006) A short mitochondrial form of p19ARF induces autophagy and caspase-independent cell death. Mol. Cell 22, 463–475.
[15] Chen, C. and Okayama, H. (1987) High-efficiency transformation of mammalian cells by plasmid DNA. Mol. Cell Biol. 7, 2745–2752.
[16] Yoneda-Kato, N., Tomoda, K., Umehara, M., Arata, Y. and Kato, J.Y. (2005) Myeloid leukemia factor 1 regulates p53 by suppressing COP1 via COP9 signalosome subunit 3. EMBO J. 24, 1739–1749.
[17] Kato, J.Y., Nakamae, I., Tomoda, K., Fukumoto, A. and Yoneda-Kato, N. (2006) Preparation and characterization of monoclonal antibodies against mouse Jab1/CSN5 protein. Hybridoma (Larchmt) 25, 342–348.
[18] Zhang, Y., Xiong, Y. and Yarbrough, W.G. (1998) ARF promotes MDM2 degradation and stabilizes p53: ARF-INK4a locus deletion impairs both the Rb and p53 tumor suppression pathways. Cell 92, 725–734.
[19] Honda, R. and Yasuda, H. (1999) Association of p19(ARF) with Mdm2 inhibits ubiquitin ligase activity of Mdm2 for tumor suppressor p53. EMBO J. 18, 22–27.
[20] Weber, J.D., Taylor, L.J., Roussel, M.F., Sherr, C.J. and Bar-Sagi, D. (1999) Nucleolar Arf sequesters Mdm2 and activates p53. Nat. Cell Biol. 1, 20–26.
[21] Weber, J.D., Kuo, M.L., Bothner, B., DiGiammarino, E.L., Kriwacki, R.W., Roussel, M.F. and Sherr, C.J. (2000) Cooperative signals governing ARF-mdm2 interaction and nucleolar localization of the complex. Mol. Cell Biol. 20, 2517–2528.
[22] Korgaonkar, C., Zhao, L., Modestou, M. and Quelle, D.E. (2002) ARF function does not require p53 stabilization or Mdm2 relocalization. Mol. Cell Biol. 22, 196–206.

[23] Bothner, B., Lewis, W.S., DiGiammarino, E.L., Weber, J.D., Bothner, S.J. and Kriwacki, R.W. (2001) Defining the molecular basis of Arf and Hdm2 interactions. J. Mol. Biol. 314, 263–277.
[24] Leng, R.P. et al. (2003) Pirh2, a p53-induced ubiquitin-protein ligase, promotes p53 degradation. Cell 112, 779–791.
[25] Dornan, D. et al. (2004) The ubiquitin ligase COP1 is a critical negative regulator of p53. Nature 429, 86–92.
[26] Stommel, J.M., Marchenko, N.D., Jimenez, G.S., Moll, U.M., Hope, T.J. and Wahl, G.M. (1999) A leucine-rich nuclear export signal in the p53 tetramerization domain: regulation of subcellular localization and p53 activity by NES masking. EMBO J. 18, 1660–1672.
[27] Mihara, M., Erster, S., Zaika, A., Petrenko, O., Chittenden, T., Pancoska, P. and Moll, U.M. (2003) p53 has a direct apoptogenic role at the mitochondria. Mol. Cell 11, 577–590.